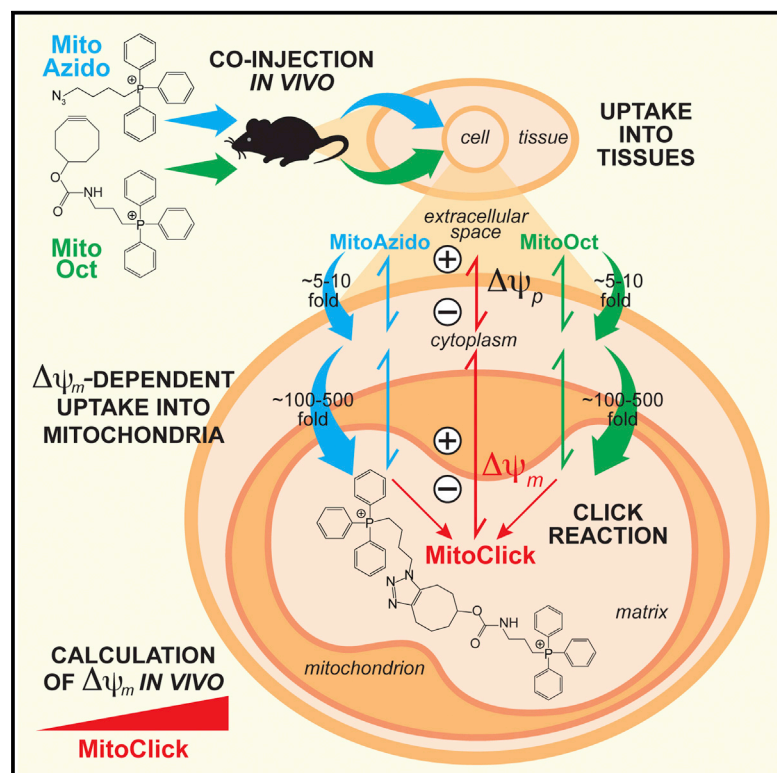


# Cell Metabolism

## Assessing the Mitochondrial Membrane Potential in Cells and In Vivo using Targeted Click Chemistry and Mass Spectrometry

### Graphical Abstract



### Authors

Angela Logan, Victoria R. Pell, Karl J. Shaffer, ..., Thomas Krieg, Robin A.J. Smith, Michael P. Murphy

### Correspondence

mpm@mrc-mbu.cam.ac.uk

### In Brief

The mitochondrial membrane potential is central to the organelle's many functions. Combining mitochondria targeted probes, click chemistry, and mass spectrometry, Logan et al. develop a highly sensitive approach to assess small changes in membrane potential in cells and in vivo, and show its utility in proof-of-principle experiments.

### Highlights

- Mass spectrometry and click chemistry can assess mitochondrial membrane potential
- This approach can be applied to investigate membrane potential in cells and in vivo
- Hypotheses dependent on small changes in membrane potential can be tested



# Assessing the Mitochondrial Membrane Potential in Cells and In Vivo using Targeted Click Chemistry and Mass Spectrometry

Angela Logan,<sup>1,9</sup> Victoria R. Pell,<sup>2,9</sup> Karl J. Shaffer,<sup>3</sup> Cameron Evans,<sup>3</sup> Nathan J. Stanley,<sup>3</sup> Ellen L. Robb,<sup>1</sup> Tracy A. Prime,<sup>1</sup> Edward T. Chouchani,<sup>1,2,4,5</sup> Helena M. Cochemé,<sup>6,7</sup> Ian M. Fearnley,<sup>1</sup> Sara Vidoni,<sup>1</sup> Andrew M. James,<sup>1</sup> Carolyn M. Porteous,<sup>3,8</sup> Linda Partridge,<sup>6</sup> Thomas Krieg,<sup>2</sup> Robin A.J. Smith,<sup>3</sup> and Michael P. Murphy<sup>1,\*</sup>

<sup>1</sup>Medical Research Council Mitochondrial Biology Unit, Hills Road, Cambridge CB2 0XY, UK

<sup>2</sup>Department of Medicine, University of Cambridge, Addenbrooke's Hospital, Hills Road, Cambridge, CB2 2QQ, UK

<sup>3</sup>Department of Chemistry, University of Otago, P.O. Box 56, Dunedin 9054, New Zealand

<sup>4</sup>Dana-Farber Cancer Institute and Department of Cell Biology, Harvard Medical School, Boston, MA 02115, USA

<sup>5</sup>Department of Cell Biology, Harvard University Medical School, Boston, MA 02115, USA

<sup>6</sup>Institute of Healthy Ageing, Department of Genetics, Evolution, and Environment, University College London, Gower Street, London WC1E 6BT, UK

<sup>7</sup>MRC Clinical Sciences Centre, Imperial College London, Du Cane Road, London W12 0NN, UK

<sup>8</sup>Department of Biochemistry, University of Otago, P.O. Box 56, Dunedin 9054, New Zealand

<sup>9</sup>Co-first author

\*Correspondence: [mmp@mrc-mbu.cam.ac.uk](mailto:mmp@mrc-mbu.cam.ac.uk)

<http://dx.doi.org/10.1016/j.cmet.2015.11.014>

This is an open access article under the CC BY-NC-ND license (<http://creativecommons.org/licenses/by-nc-nd/4.0/>).

## SUMMARY

The mitochondrial membrane potential ( $\Delta\psi_m$ ) is a major determinant and indicator of cell fate, but it is not possible to assess small changes in  $\Delta\psi_m$  within cells or in vivo. To overcome this, we developed an approach that utilizes two mitochondria-targeted probes each containing a triphenylphosphonium (TPP) lipophilic cation that drives their accumulation in response to  $\Delta\psi_m$  and the plasma membrane potential ( $\Delta\psi_p$ ). One probe contains an azido moiety and the other a cyclooctyne, which react together in a concentration-dependent manner by “click” chemistry to form MitoClick. As the mitochondrial accumulation of both probes depends exponentially on  $\Delta\psi_m$  and  $\Delta\psi_p$ , the rate of MitoClick formation is exquisitely sensitive to small changes in these potentials. MitoClick accumulation can then be quantified by liquid chromatography-tandem mass spectrometry (LC-MS/MS). This approach enables assessment of subtle changes in membrane potentials within cells and in the mouse heart in vivo.

## INTRODUCTION

The mitochondrial membrane potential ( $\Delta\psi_m$ ) is central to the organelle's many functions (Nicholls and Ferguson, 2013). As electrons pass down the respiratory chain to oxygen, the difference in reduction potential drives proton pumping across the inner membrane, generating a proton electrochemical potential gradient comprising a pH gradient ( $\sim 0.8$  pH units/50 mV, basic

inside) and a  $\Delta\psi_m$  ( $\sim 120$ – $180$  mV, negative inside); thus  $\Delta\psi_m$  is by far the dominant component. The central function of  $\Delta\psi_m$  is to drive ATP synthesis by oxidative phosphorylation, and its magnitude is set by the balance between its generation and its consumption by ATP synthesis and other dissipative processes (Figure 1A), making  $\Delta\psi_m$  a sensitive indicator of cellular energetics.  $\Delta\psi_m$  can decrease due to elevated ATP production or thermogenesis, or from mitochondrial dysfunction, while  $\Delta\psi_m$  can increase due to diminished ATP synthesis or an upregulation of proton pumping. Such increases occur in apoptosis and cancer (Smith et al., 2012; Wallace et al., 2010). An increase in  $\Delta\psi_m$  is also a key driver of mitochondrial ROS production in pathology and redox signaling (Murphy, 2009). Consequently, many biomedically central phenomena are associated with subtle changes in  $\Delta\psi_m$ , and the ability to quantify these alterations in vivo and in cells should enable mechanistic insights and facilitate novel approaches to diagnosis and therapies (Figure 1A).

Changes in  $\Delta\psi_m$  within cells can be assessed using fluorescent or radiolabeled lipophilic cations; however, these approaches are insensitive to small changes (Davidson et al., 2007; Perry et al., 2011) and can only be used in restricted situations in vivo (Davidson et al., 2007; Sack, 2006). Hence we have developed a sensitive method to assess small changes in  $\Delta\psi_m$  and  $\Delta\psi_p$ , in cells and in vivo. For this we direct probes to mitochondria using a triphenylphosphonium (TPP) lipophilic cation (Ross et al., 2005; Smith et al., 2011, 2012). The large hydrophobic surface area of the TPP cation enables its rapid, several-hundred-fold accumulation into cells in response to the  $\Delta\psi_p$  and from there into mitochondria in response to  $\Delta\psi_m$  (Ross et al., 2005). To assess relative changes in  $\Delta\psi_m$  and  $\Delta\psi_p$ , we administer two TPP compounds simultaneously, both of which accumulate within mitochondria and react together to form a stable product (Figure 1B). The reaction rate is proportional to the local concentrations of both reactants, each of which accumulates in

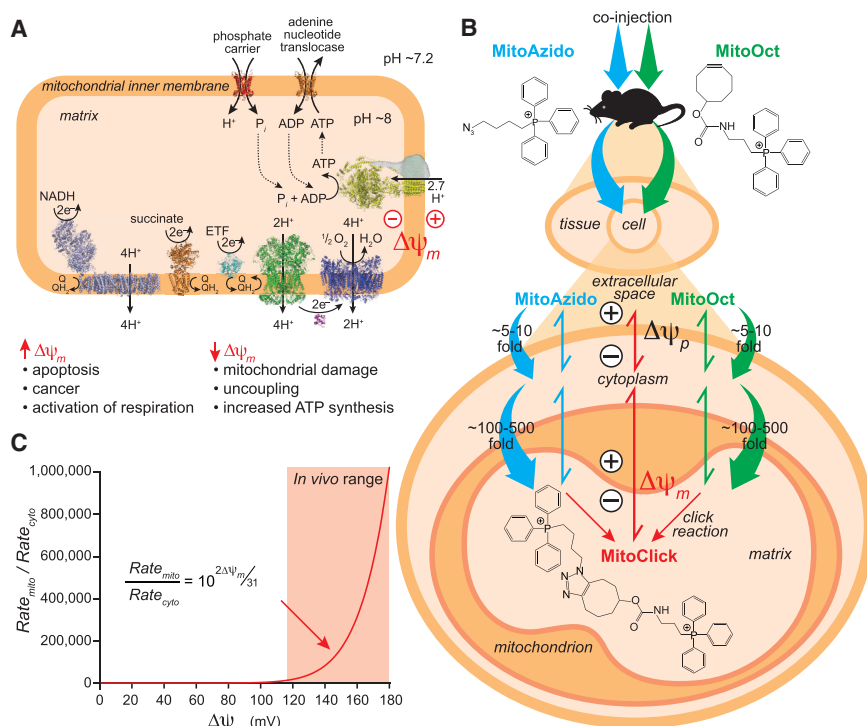


**Figure 1. Rationale for Mitochondria-Targeted Click Chemistry to Assess  $\Delta\psi_m$**

(A)  $\Delta\psi_m$  in vivo. This shows a mitochondrion with the respiratory chain generating  $\Delta\psi_m$  by pumping protons across the inner membrane. The  $\Delta\psi_m$  is used to synthesize ATP. Situations in which the steady-state level of  $\Delta\psi_m$  within cells and in vivo change are indicated.

(B) The structures of MitoAzido and MitoOct are shown along with their uptake into the cell in response to the plasma membrane potential ( $\Delta\psi_p$ ) and then into mitochondria in response to the  $\Delta\psi_m$  across the inner membrane in vivo, followed by their click reaction together to form MitoClick as a regioisomeric mixture.

(C) The rate of MitoClick formation in the mitochondrial matrix divided by the rate in the cytosol as a function of  $\Delta\psi_m$ , with the cytosolic concentrations of MitoAzido and MitoOct held constant. Equation 2, which describes this curve, is shown. See also Figure S1.

Therefore every 1 mV  $\Delta\psi_m$  increase accelerates mitochondrial MitoClick formation relative to that in the cytosol ~800-fold at 120 mV and ~80,000-fold at 180 mV. This leads to an 8% compounded increase in MitoClick formation per mV, making very small relative changes in  $\Delta\psi_m$  easy to assess (Figure 1C). It is essential to note that, as with all methods dependent on lipophilic cation accumulation, the accumulation of MitoClick will also be sensitive to small changes in  $\Delta\psi_p$ . Alteration of mitochondrial, cell, and extracellular volumes, and excretion and binding, will also affect the rate of MitoClick formation. Consequently, while in all cases small changes in  $\Delta\psi_m$  will dramatically alter MitoClick formation rate, it is vital to consider the many confounding factors that could impact on measurements.

To quantify the amount of MitoClick formed within tissues, we use liquid chromatography-tandem mass spectrometry (LC-MS/MS) relative to deuterated internal standards, which enables sensitive detection of TPP probes (Cochemé et al., 2011). Here we describe the development and application of mitochondria-targeted click reagents to assess small changes of  $\Delta\psi_m$  in cells and in vivo.

To quantify the amount of MitoClick formed within tissues, we use liquid chromatography-tandem mass spectrometry (LC-MS/MS) relative to deuterated internal standards, which enables sensitive detection of TPP probes (Cochemé et al., 2011). Here we describe the development and application of mitochondria-targeted click reagents to assess small changes of  $\Delta\psi_m$  in cells and in vivo.

## RESULTS AND DISCUSSION

### Uptake of MitoOct and MitoAzido Forms MitoClick within Energized Mitochondria

The syntheses of MitoOct and MitoAzido are shown in Figures S1A and S1B. Reaction of MitoOct with MitoAzido gave only MitoClick (Figure S1C) as a 1:1 mixture of regioisomers, determined by <sup>1</sup>H-NMR and high-resolution mass spectrometry (Supplemental Information). RP-HPLC also showed that MitoOct and MitoAzido reacted together to form MitoClick under biological conditions (Figure 2A). We used an ion-selective electrode to show that MitoOct and MitoAzido were taken up by energized mitochondria and released upon dissipation of  $\Delta\psi_m$  with the uncoupler carbonylcyanide-*p*-trifluoromethoxyphenylhydrazone

mitochondria  $\sim 10^2$ - to  $10^3$ -fold driven by  $\Delta\psi_p$  and  $\Delta\psi_m$ , hence product formation there will be  $\sim 10^4$ - to  $10^6$ -fold faster than that in the cytosol and will be extremely sensitive to small changes in  $\Delta\psi_m$  and  $\Delta\psi_p$  (Figure 1B).

For this to work, the two probes must react specifically with each other and not with other biomolecules. To achieve this, we used “click” chemistry, which utilizes azido and alkyne groups, which couple *ex vivo* under Cu(I) catalysis (Kolb et al., 2001). To enable the reaction to occur in vivo without catalysis, Bertozzi developed strained cyclooctynes (Agard et al., 2004; Jewett and Bertozzi, 2010). Therefore we prepared TPP compounds containing cyclooctyne (MitoOct) and azido (MitoAzido) moieties, which react together to form MitoClick (Figure 1B).

The rate of the reaction of MitoOct with MitoAzido to form MitoClick is

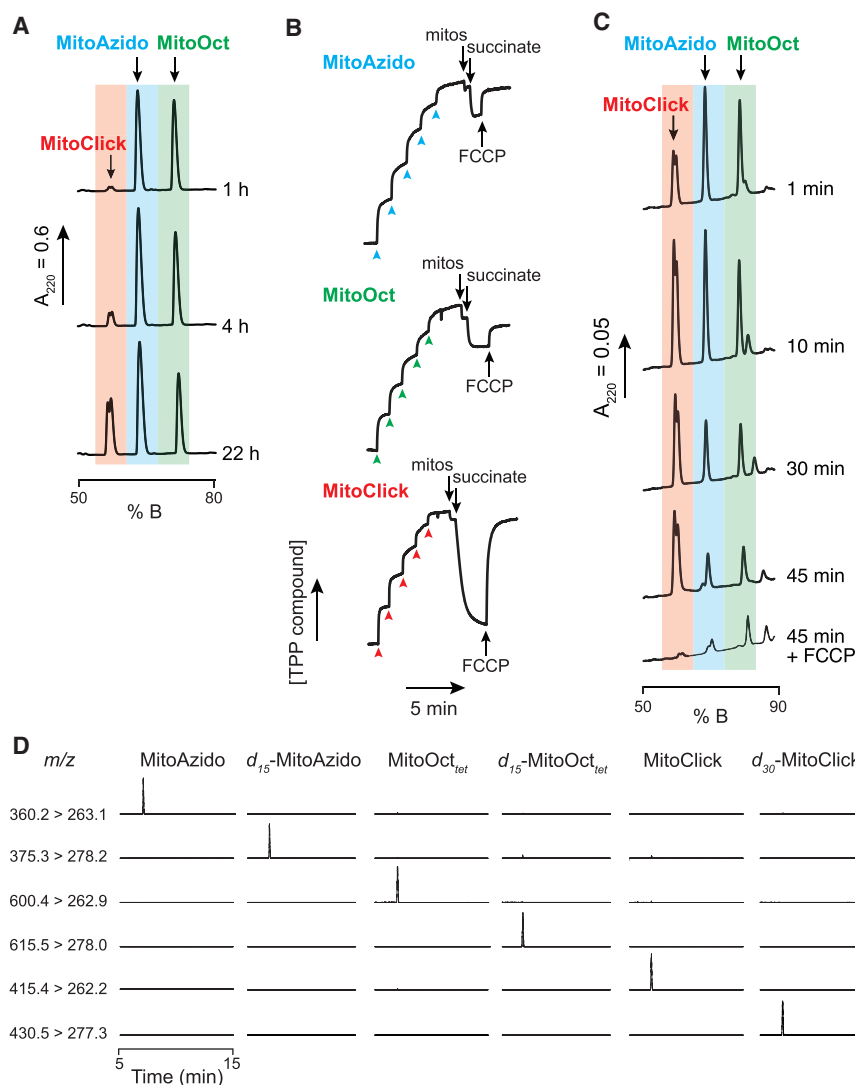
$$\text{Rate}_{\text{MitoClick}} = k[\text{MitoAzido}][\text{MitoOct}] \quad (1)$$

where  $k$  is the second order rate constant. As shown in Supplemental Information, available online, the ratio of the rates of MitoClick formation in mitochondria and cytosol is

$$\frac{\text{Rate}_{\text{Mito}}}{\text{Rate}_{\text{Cyto}}} = 10^{2\Delta\psi_m/2.303RT} = 10^{2\Delta\psi_m/31} \quad (2)$$

Thus, there is an exponential dependence of the rate enhancement on  $\Delta\psi_m$  over the biologically relevant range from 120 to 180 mV (Figure 1C) (Brand and Murphy, 1987; Porteous et al., 1998), assuming no confounding changes in  $\Delta\psi_p$ . Differentiation of Equation 2 gives

$$\frac{d\left(\frac{\text{Rate}_{\text{Mito}}}{\text{Rate}_{\text{Cyto}}}\right)}{d\Delta\psi_m} = \frac{\text{Ln}10}{31} 10^{2\Delta\psi_m/31} \quad (3)$$



(FCCP) (Figure 2B). The uptake for MitoOct or MitoAzido ( $\sim 1\text{--}1.5$  nmol/mg protein) (Figure 2B), corresponds to 2–3 mM in the matrix (assuming  $\sim 0.5$   $\mu\text{L}/\text{mg}$  protein [Ross et al., 2008] and uncorrected for binding),  $\sim 1,000$ -fold greater than the external concentration ( $\sim 3$   $\mu\text{M}$ ), consistent with  $\Delta\psi_m$ -dependent uptake. MitoClick mitochondrial uptake was  $\sim 3\text{--}3.5$  nmol/mg protein (Figure 2B), about 6–7 mM in the matrix,  $\sim 10,000$ -fold greater than the external concentration ( $\sim 0.5$   $\mu\text{M}$ ), more than its monocationic precursors, as expected for a dication (Ross et al., 2006).

To see if MitoClick formation was enhanced by mitochondrial accumulation of its precursors, we incubated MitoOct and MitoAzido with mitochondria and measured MitoClick formation (Figure 2C). There was extensive MitoClick generation after 1 min with mitochondria (Figure 2C), compared to negligible formation over 1 hr without mitochondria (Figure 2A), and this MitoClick formation was prevented by FCCP (Figure 2C). Therefore, both MitoOct and MitoAzido are extensively accumulated by mitochondria in response to  $\Delta\psi_m$ , dramatically increasing the rate of MitoClick formation.

## Figure 2. Reaction of MitoOct and MitoAzido to Form MitoClick in Mitochondria

(A) MitoOct and MitoAzido (10 nmol of each) were incubated in 250  $\mu\text{L}$  KCl medium at room temperature for the indicated times and then analyzed by RP-HPLC. The double peak for MitoClick by RP-HPLC is due to the formation of the two MitoClick regioisomers.

(B) Isolated mitochondria were incubated in the chamber of an ion-selective electrode, and the response was calibrated by  $5 \times 1$   $\mu\text{M}$  successive additions of MitoAzido, MitoOct, or MitoClick. Where indicated mitochondria, succinate and FCCP were added.

(C) Mitochondria were incubated with MitoAzido (5  $\mu\text{M}$ ) and MitoOct (5  $\mu\text{M}$ ) for the indicated times, pelleted, and extracted with ACN and the extract analyzed by RP-HPLC.

(D) Typical LC-MS/MS chromatograms showing the  $m/z$  transitions measured simultaneously for 50 nM each of MitoAzido,  $d_{15}$ -MitoAzido, MitoOct<sub>tet</sub>,  $d_{15}$ -MitoOct<sub>tet</sub>, MitoClick, and  $d_{30}$ -MitoClick. Traces are normalized to the maximum total ion count measured during that experiment. See also Figure S2 and Tables S1 and S2.

## LC-MS/MS Analysis of MitoClick Formation from MitoOct and MitoAzido

The measurement of MitoClick formation *in vivo* necessitates LC-MS/MS detection, because RP-HPLC is too insensitive. However, LC-MS/MS requires solvent extraction followed by evaporation under vacuum (Cochemé et al., 2011), greatly concentrating unreacted MitoAzido and MitoOct which would lead to extensive *ex vivo* MitoClick formation. To prevent this we used a blocking reagent, 3-phenyl-1,2,4,5-tetrazine (Tet), which

reacts very rapidly with MitoOct to generate MitoOct<sub>tet</sub> (Figure S2A) (Karver et al., 2012). The reaction of Tet with MitoOct ( $k \sim 12.1 \times 10^6 \text{ M}^{-1}\text{s}^{-1}$  [Balcar et al., 1983]) is  $\sim 10^8$ -fold faster than that for MitoAzido ( $k \sim 0.1\text{--}0.2 \text{ M}^{-1}\text{s}^{-1}$ ). Including Tet in the extraction solution prevented artifactual MitoClick formation (Figure S2B; Table S1).

To establish LC-MS/MS assays, we fragmented MitoClick, MitoOct<sub>tet</sub>, and MitoAzido and analyzed the product ions to select mass transitions for quantification (Table S2). These transitions are selective for the intended species by LC-MS/MS (Figure 2D). From these, standard curves were established for MitoAzido, MitoOct<sub>tet</sub> and MitoClick in tissue homogenates with detection down to  $\sim 1\text{--}5$  pmol per g wet weight tissue (Figure S2C). This approach was used to assess the rate of reaction of MitoOct and MitoAzido in solution (Figures S2D and S2E).

## Analysis of MitoClick Formation in Mitochondria and Cells

Formation of MitoClick from MitoAzido and MitoOct in isolated mitochondria was assessed by LC-MS/MS (Figure 3A). The



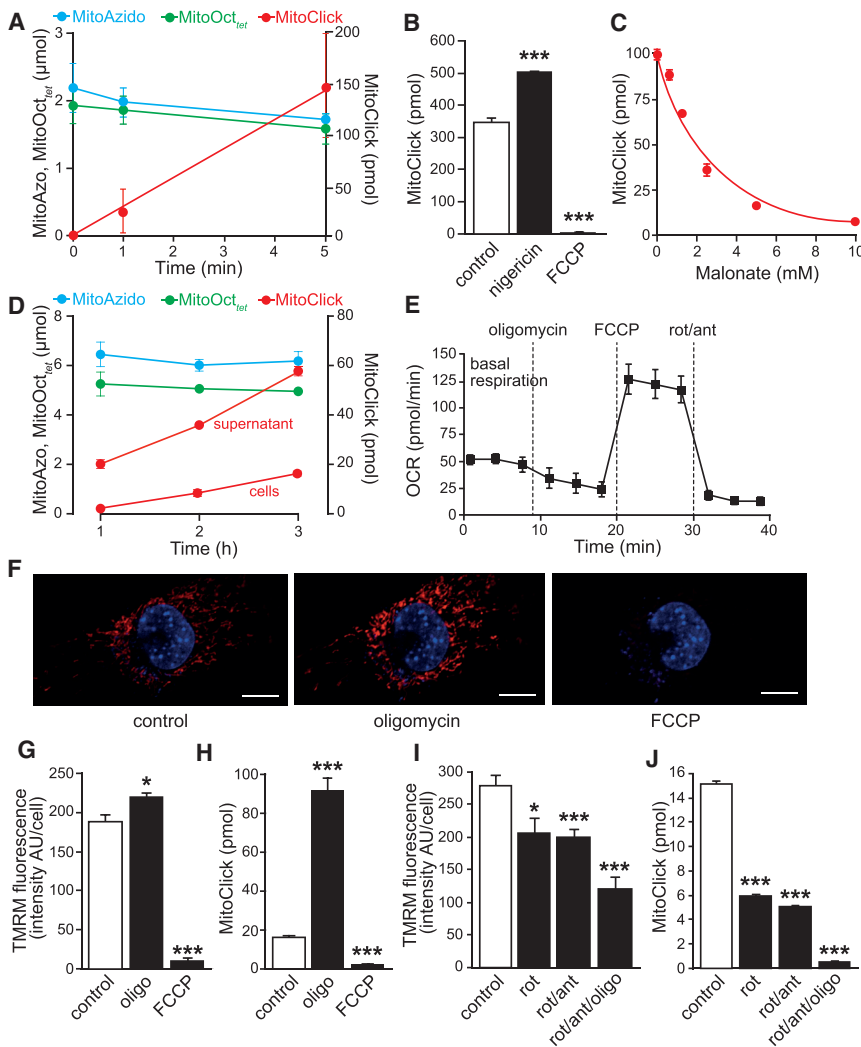


**Figure 3. Assessment of MitoClick Formation by LC-MS/MS in Mitochondria and Cells**

(A) Detection of MitoAzido, MitoOct<sub>tet</sub>, and MitoClick in mitochondria. Rat liver mitochondria (1 mg protein/mL) were incubated with 5  $\mu$ M of MitoAzido and MitoOct in KCl medium at 37°C. Samples were removed at the indicated times, and mitochondria were pelleted, quenched with Tet, and then extracted and analyzed by LC-MS/MS. Data are means  $\pm$  SEM of three separate mitochondrial preparations.

(B) Detection of MitoClick in mitochondria. Rat liver mitochondria were incubated as in (A) for 5 min  $\pm$  FCCP (500 nM) or nigericin.

(C) Effect of malonate on MitoClick formation in mitochondria. Rat liver mitochondria were incubated as in (A) for 5 min with increasing concentrations of malonate. Samples were removed, quenched with Tet, then extracted and analyzed by LC-MS/MS. Data are means  $\pm$  SEM of three replicates.

(D) Detection of MitoAzido, MitoOct<sub>tet</sub>, and MitoClick in cells. C2C12 cells were incubated with 5  $\mu$ M each of MitoAzido and MitoOct for up to 3 hr. The supernatant was removed and the cell layer was scraped into PBS, and both were quenched with Tet, extracted, and analyzed by LC-MS/MS. Data are means  $\pm$  SEM of three independent experiments.

(E) Oxygen consumption rate (OCR) measured in C2C12 cells. Where indicated, oligomycin (4  $\mu$ M), FCCP (2  $\mu$ M), and rotenone/antimycin (4  $\mu$ g/mL) were added. Each point is the mean  $\pm$  range of measurements on two wells.

(F) Detection of changes in  $\Delta\psi_m$  using TMRM staining in cells. C2C12 cells were treated with 100 nM TMRM and 500 ng/mL Hoescht 33342 for 15 min prior to imaging. Cells were imaged on a temperature-control stage of a Nikon Eclipse Ti microscope using 63 $\times$  oil immersion lens. Where indicated, additions of oligomycin (4  $\mu$ M) and FCCP (2  $\mu$ M) were made directly to the cultured cells.

(G) Assessment of changes in  $\Delta\psi_m$  using TMRM staining in cells. Fluorescence intensity of eight cells per experiment evaluated using Nikon elements software. Data shown are means  $\pm$  SEM of three independent experiments.

(H) Effect of FCCP and oligomycin on MitoClick formation in cells. C2C12 cells were incubated with 5  $\mu$ M each of MitoAzido and MitoOct alone or with oligomycin (1  $\mu$ g/mL) or FCCP (2  $\mu$ M) as indicated for 3 hr. The cell layer was scraped into PBS, quenched with Tet, extracted, and analyzed by LC-MS/MS.

(I) Assessment of changes in  $\Delta\psi_m$  due to mitochondrial inhibitors using TMRM staining in cells. Fluorescence intensity of eight cells per experiment after 15 min incubation was assessed as in (G). Incubations contained no further additions (control), rotenone (4  $\mu$ g/mL) (rot), rotenone (4  $\mu$ g/mL), and antimycin (4  $\mu$ g/mL) (rot/ant) or rotenone (4  $\mu$ g/mL), antimycin (4  $\mu$ g/mL), and oligomycin (1  $\mu$ g/mL) (rot/ant/olig). Data shown are means  $\pm$  SEM of three independent experiments.

(J) Effect of mitochondrial inhibitors on MitoClick formation in cells. C2C12 cells were incubated with 5  $\mu$ M each of MitoAzido and MitoOct alone (cont) or rotenone (4  $\mu$ g/mL) (rot), rotenone (4  $\mu$ g/mL), and antimycin (4  $\mu$ g/mL) (rot/ant) or rotenone (4  $\mu$ g/mL), antimycin (4  $\mu$ g/mL), and oligomycin (1  $\mu$ g/mL) (rot/ant/olig) as indicated for 3 hr. The cell layer was scraped into PBS, quenched with Tet, extracted, and analyzed by LC-MS/MS. Data are means  $\pm$  SEM of three independent experiments. \* $p$  < 0.05, \*\* $p$  < 0.01, \*\*\* $p$  < 0.001 assessed by Student's  $t$  test relative to untreated control.

levels of MitoOct<sub>tet</sub> and MitoAzido were stable over 5 min, while MitoClick increased, consistent with formation in mitochondria (Figure 3A). Abolition of  $\Delta\psi_m$  with FCCP prevented MitoClick formation, while increasing  $\Delta\psi_m$  with nigericin increased its generation (Figure 3B). Gradually decreasing  $\Delta\psi_m$  with the respiratory inhibitor malonate led to a corresponding decrease in MitoClick (Figure 3C). Thus MitoClick formation in mitochondria is sensitive to small changes in  $\Delta\psi_m$ .

When we incubated MitoAzido and MitoOct with cells, MitoClick increased over time in both the supernatant and cells (Figure 3D). To see how MitoClick formation responded to small

changes of  $\Delta\psi_m$ , we assessed  $\Delta\psi_m$  alterations that are likely to occur in cells, illustrated by oxygen consumption rate (OCR) measurements (Figure 3E). Under basal respiration, mitochondria make ATP and have a submaximal  $\Delta\psi_m$ ; oligomycin inhibits ATP synthesis maximizing  $\Delta\psi_m$  and decreasing OCR; finally, FCCP abolishes  $\Delta\psi_m$  and maximizes OCR (Figure 3E). The associated subtle changes in  $\Delta\psi_m$  are less easily assessed, as is illustrated using a current benchmark for  $\Delta\psi_m$  investigation, the fluorescence of tetramethylrhodamine (TMRM) in nonquenching mode (Figures 3F and 3G). Increasing  $\Delta\psi_m$  from its normal value to its maximum with oligomycin gave only a small change in

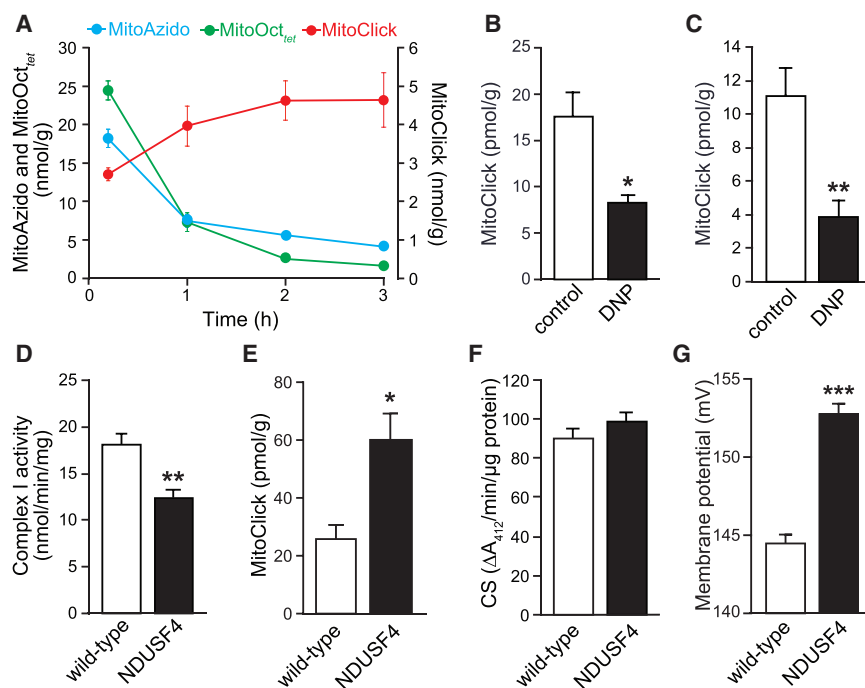


**Figure 4. Assessment of MitoClick Formation by LC-MS/MS in Mice**

(A) Detection of MitoAzido, MitoOct<sub>tet</sub>, and MitoClick in mouse heart. Mice were injected i.v. with 50 nmol each of MitoAzido and MitoOct, and after the indicated times the heart was removed and MitoAzido, MitoOct<sub>tet</sub>, and MitoClick were analyzed by LC-MS/MS. Data are means ± SEM of three mice per time point. See also Figure S3.

(B and C) Effect of DNP on MitoClick formation within the mouse heart. Mice were injected i.v. with 10 nmol each of MitoAzido and MitoOct at various times after DNP administration, then 1 min later the heart was removed and MitoAzido, MitoOct<sub>tet</sub>, and MitoClick analyzed by LC-MS/MS. In (B) MitoAzido and MitoOct were injected 15 min after i.p. administration of DNP (1 mg/kg). Data are means ± SEM of eight mice. In (C) mice were administered DNP (5 mg/kg) by oral gavage, and 60 min later MitoAzido and MitoOct<sub>tet</sub> were injected. Data are means ± SEM of five mice.

(D) Complex I activity in the hearts of *Ndufs4*-null mice. Heart mitochondria from *Ndufs4*-null and wild-type control mice were isolated and the complex I activity was measured. Data are means ± SEM of four independent mitochondrial preparations.

(E) MitoClick formation in the heart of *Ndufs4*-null mice. Mice were injected with MitoAzido and MitoOct and after 1 min MitoClick was analyzed as in (A). Data are mean ± SEM of four mice.

(F) Citrate synthase activity in the hearts of *Ndufs4*-null mice. Heart mitochondria from *Ndufs4*-null and wild-type control mice were isolated and citrate synthase activity was measured. Data are means ± SEM of 4 independent mitochondrial preparations.

(G)  $\Delta\psi_m$  of isolated heart mitochondria from *Ndufs4*-null mice. Heart mitochondria from *Ndufs4*-null and wild-type control mice were incubated with 10 mM succinate, and  $\Delta\psi_m$  was measured from the distribution of [<sup>3</sup>H]-TPMP. Data are means ± SEM of six independent mitochondrial preparations. See also Figure S3.

fluorescence (Figures 3F and 3G). In contrast, the same increase in  $\Delta\psi_m$  dramatically enhanced MitoClick formation (Figure 3H). Similarly, inhibition of respiration by rotenone and/or antimycin showed a far greater change in MitoClick than TMRM (Figures 3I and 3J). Subsequent addition of oligomycin further lowered  $\Delta\psi_m$  by inhibiting proton pumping by the ATP synthase (Figures 3I and 3J). Therefore MitoClick formation is exquisitely sensitive to small changes in  $\Delta\psi_m$  within cells (Figure 1C).

#### Use of MitoClick Formation to Assess Relative Changes in $\Delta\psi_m$ within Mice

Methods to assess subtle changes in  $\Delta\psi_m$  in mice in vivo have long been sought. TPP can target a wide range of compounds to mitochondria within mice, following intravenous (i.v.) administration with rapid (minutes) mitochondrial uptake within the heart, liver, and kidney (Porteous et al., 2010; 2013; Smith et al., 2011, 2012). MitoAzido and MitoOct could be given safely i.v. by tail vein injection to mice; therefore over the next 3 hr we measured their levels and those of MitoClick in the heart (Figure 4A). There was an initial increase in MitoOct and MitoAzido content, as expected due to the rapid uptake of TPP compounds by the heart in response to  $\Delta\psi_p$  and  $\Delta\psi_m$  (Porteous et al., 2010, 2013). These compounds were lost with half-lives of ~0.8 hr, due to their re-equilibration across membranes followed by excretion in the urine and bile (Smith et al., 2011). There was rapid initial MitoClick formation, due to the high MitoAzido and MitoOct

mitochondrial concentrations immediately following injection (Figure 4A). MitoClick formation was sustained for a short time and then stopped, as the precursors became depleted (Figure 4A). MitoClick was retained longer due to its double positive charge (Ross et al., 2006) (Figure 4A). The kidney showed less MitoAzido and MitoOct uptake than the heart, and the apparent rate of excretion was slower, consistent with redistribution from other organs (Figure S3B). There was uptake of MitoAzido and MitoOct into the liver (Figure S3B); however, MitoOct and MitoClick were rapidly lost from this tissue, probably due to excretion by the biliary pathway (Porteous et al., 2013). These findings suggest that the rapid initial formation of MitoClick in the heart following a single i.v. injection of its precursors may be used to infer changes in  $\Delta\psi_p$  and  $\Delta\psi_m$  in vivo. However, it is important to note that the factors that determine MitoClick formation in vivo are quite different from those that dominate for cells in culture. In vivo, MitoOct and MitoAzido do not have the opportunity to equilibrate with  $\Delta\psi_p$  and  $\Delta\psi_m$  as they do in cells. In contrast, kinetic factors such as blood flow, tissue uptake, and excretion determine the initial uptake into cells and mitochondria. Even so, the local concentration of MitoOct and MitoAzido within mitochondria by  $\Delta\psi_p$  and  $\Delta\psi_m$  suggests that the initial formation of MitoClick in tissues reports on changes in these potentials.

The response of MitoClick formation to changes in  $\Delta\psi_m$  in the heart was evaluated using the uncoupler 2,4-dinitrophenol

(DNP). Uncoupling by DNP leads to pathological heat generation in vivo and is known to decrease  $\Delta\psi_m$  (Jucker et al., 2000). DNP decreased the formation of MitoClick indicating that this approach can be used to assess changes in  $\Delta\psi_m$  within the heart in vivo (Figures 4B and 4C). MitoClick could be used to assess the toxic effects of DNP and assist in the development of safer formulations (Perry et al., 2015); however, we note that the response of MitoClick formation in vivo to DNP administration route and dose was not straightforward, presumably due to DNP distribution and compensatory changes in mitochondrial respiration and  $\Delta\psi_m$ . Next, we used MitoClick to assess whether there was a change in  $\Delta\psi_m$  in a mouse model of heart mitochondrial dysfunction. We used a heart-specific *Ndufs4*-null strain (Chouchani et al., 2014; Karamanlidis et al., 2013; Sterky et al., 2012). *Ndufs4* encodes an 18 kDa subunit of respiratory complex I that plays a role in assembly and/or stability of the complex (Karamanlidis et al., 2013). The *Ndufs4*-null mice had an ~50% decrease in complex I activity in the heart, and developed severe cardiomyopathy (Chouchani et al., 2014; Karamanlidis et al., 2013). We confirmed the decreased complex I activity (Figure 4D), and therefore expected to find a decrease in  $\Delta\psi_m$  in the heart due to defective proton pumping. To our great surprise, MitoClick formation was actually elevated compared to control mice (Figure 4E). One possibility was that MitoClick formation increased within *Ndufs4*-null hearts due to a compensatory increase in mitochondrial content. However, the mitochondrial marker enzyme citrate synthase showed no such increase (Figure 4F). To see if there was a change in mitochondrial energetics, we assessed isolated heart mitochondria in vitro, and this showed that heart mitochondria from the *Ndufs4*-null mice had a higher  $\Delta\psi_m$  when respiring on succinate (Figure 4G), suggesting a compensatory upregulation of  $\Delta\psi_m$  generation from complex II-linked substrates to counteract the complex I-linked defect in the hearts of *Ndufs4*-null mice. This surprising result inadvertently provided a good test for MitoClick and showed that it can assess unexpected small changes in  $\Delta\psi_m$  in vivo. However, it is important to note that further work is required to determine whether the relative change in MitoClick formation in these mice could be in part due to changes in  $\Delta\psi_p$  or mitochondrial volume. Even so, these findings with the *Ndufs4*-null mice show how MitoClick can contribute to investigating subtle changes to  $\Delta\psi_m$  in the heart in vivo.

## Conclusion

As  $\Delta\psi_m$  is central to mitochondrial function and dysfunction, subtle changes are of considerable significance for cell fate and health. The difficulty of assessing small changes in  $\Delta\psi_m$  in cells and in vivo is a major impediment to understanding normal and pathological mitochondrial function in a range of biomedically important situations. Here we have developed a highly sensitive approach that can contribute to the assessment of  $\Delta\psi_m$  in cells and in vivo, and shown its utility in proof of principle experiments.

A unique aspect of the approach is that it utilizes  $\Delta\psi_m$ - and  $\Delta\psi_p$ -dependent uptake and reaction together of two cations to form a diagnostic product, MitoClick. Consequently, the rate of MitoClick formation is particularly sensitive to small changes in  $\Delta\psi_m$  and  $\Delta\psi_p$  due to the logarithmic relationship of uptake of both cations to these potentials. Transformation of potential measurement from a reversible compound distribution to an

irreversible reaction rate circumvents the hitherto intractable problem of compound redistribution during sample work up. Consequently, changes in  $\Delta\psi_m$  and  $\Delta\psi_p$  can be assessed in vivo, within whole organs or organisms, and the MitoClick approach opens up new ways of exploring subtle mitochondrial changes.

There are constraints to this approach that should be borne in mind. The first is that uptake of MitoAzido and MitoOct within mitochondria will also be affected by  $\Delta\psi_p$ ; therefore changes in this variable must also be considered before concluding that MitoClick formation is related to an alteration to  $\Delta\psi_m$ . A further point is that MitoClick formation is the weighted mean of all mitochondria analyzed, and therefore gives average values of  $\Delta\psi_m$  and  $\Delta\psi_p$  in the sample. Complementary methods will be required to assess whether  $\Delta\psi_m$  or  $\Delta\psi_p$  changes in individual cells or mitochondria. It is also important to consider whether changes in MitoClick formation are influenced by mitochondrial content, as was addressed herein by measurement of a marker enzyme. A related consideration is that the local rate of formation of MitoClick will be affected by changes in the organelle volume. Therefore, although MitoClick formation is exquisitely sensitive to subtle changes in  $\Delta\psi_m$ , this very sensitivity means that we must be cautious in ascribing changes in MitoClick formation solely to  $\Delta\psi_m$ . However, these limitations apply to most methods routinely used to assess  $\Delta\psi_m$  in cells.

The concentration of two TPP compounds simultaneously within mitochondria to assemble a new compound suggests that mitochondria can be used as a “reaction chamber.” This could facilitate the generation of new bioactive, therapeutic, or toxic compounds locally within mitochondria, but with the precursors having minimal effects. This approach has been suggested previously, but using nonspecific functions (Rideout, 1994; Rotenberg et al., 1991); thus the development of TPP-conjugated click reagents opens up a new methodology for future development.

To conclude, we have shown that it is possible to assess small changes in  $\Delta\psi_m$  and  $\Delta\psi_p$  in cells in culture and in vivo using of mitochondria-targeted click reagents. This development opens up many new possibilities for assessing changes in these potentials in physiological and pathological processes.

## EXPERIMENTAL PROCEDURES

### Synthesis and In Vitro Analysis of MitoAzido, MitoOct, and MitoClick

The syntheses and characterization of MitoAzido, MitoOct, and MitoClick and their deuterated internal standards (IS) are described in the [Supplemental Information](#).

### Cell Culture

C2C12 cells were maintained in Dulbecco's modified Eagle's medium (DMEM; Invitrogen) supplemented with 10% FCS. To assess  $\Delta\psi_m$  by fluorescent microscopy, we used TMRM as described in the [Supplemental Information](#).

### Mouse Experiments

All animal experiments were carried out in accordance with the UK Animals (Scientific Procedures) Act 1986 and the University of Cambridge Animal Welfare Policy. For the time course studies, male 8- to 10-week-old C57BL/6 mice were used. The heart-specific *Ndufs4*-null strain was a gift from Nils-Göran Larsen, Köln (Chouchani et al., 2014; Sterky et al., 2012). Mice were administered MitoOct and MitoAzido by tail vein injection and were then killed by cervical dislocation with tissues being isolated and snap-frozen on liquid nitrogen. MitoOct, MitoAzido, and MitoClick were extracted from the mouse tissues as described in the [Supplemental Information](#).

### LC-MS/MS Analysis

Samples were analyzed by LC-MS/MS with multiple reaction monitoring in positive ion mode after reverse-phase separation on an I-class Acquity LC attached to a Xevo TQ-S triple quadrupole mass spectrometer (Waters), analyzed using MassLynx software. Standard curves were prepared and processed in parallel using the appropriate biological material or buffer spiked with  $d_{15}$ -MitoOct,  $d_{15}$ -MitoAzido, and  $d_{30}$ -MitoClick ISs and various amounts of MitoOct<sub>tet</sub>, MitoAzido, and MitoClick. Standard curves for the response of MitoOct<sub>tet</sub>, MitoAzido, and MitoClick relative to its deuterated IS against concentration were linear over the range 1–1,000 pmol with  $R^2$  routinely >0.99 (see Figure S3D).

### SUPPLEMENTAL INFORMATION

Supplemental Information includes three figures, two tables, supplemental calculations, and Supplemental Experimental Procedures and can be found with this article online at <http://dx.doi.org/10.1016/j.cmet.2015.11.014>.

### AUTHOR CONTRIBUTIONS

A.L. developed and carried out the mass spectrometric analyses. K.J.S., C.E., and N.J.S. performed the chemical syntheses; R.A.J.S. supervised. T.A.P., S.V., and E.L.R. carried out the in vitro experiments. V.R.P., C.M.P., and E.T.C. carried out the mouse experiments; T.K. supervised. I.M.F. helped in analysis of the mass spectrometry data. H.M.C., L.P., and A.M.J. provided conceptual advice. M.P.M., A.L., and R.A.J.S. directed the project. M.P.M. oversaw the manuscript preparation.

### ACKNOWLEDGMENTS

This work was supported by the MRC (UK) (MC-A070-5PS30), the Biotechnology and BSRC (UK) (BB/D020786/1), the Foundation for Research Science and Technology (NZ), the British Heart Foundation (BHF-PG12/42/29655), and the Human Frontiers Science Program (long-term fellowship to E.T.C.).

Received: June 22, 2015

Revised: September 2, 2015

Accepted: November 15, 2015

Published: December 17, 2015

### REFERENCES

- Agard, N.J., Prescher, J.A., and Bertozzi, C.R. (2004). A strain-promoted [3 + 2] azide-alkyne cycloaddition for covalent modification of biomolecules in living systems. *J. Am. Chem. Soc.* *126*, 15046–15047.
- Balcar, J., Chrisam, G., Huber, F.X., and Sauer, J. (1983). Reactivity of nitrogen heterocycles with cyclooctyne as dienophile. *Tetrahedron Lett.* *24*, 1481–1484.
- Brand, M.D., and Murphy, M.P. (1987). Control of electron flux through the respiratory chain in mitochondria and cells. *Biol. Rev. Camb. Philos. Soc.* *62*, 141–193.
- Chouchani, E.T., Methner, C., Buonincontri, G., Hu, C.H., Logan, A., Sawiak, S.J., Murphy, M.P., and Krieg, T. (2014). Complex I deficiency due to selective loss of Ndufs4 in the mouse heart results in severe hypertrophic cardiomyopathy. *PLoS ONE* *9*, e94157.
- Cochemé, H.M., Quin, C., McQuaker, S.J., Cabreiro, F., Logan, A., Prime, T.A., Abakumova, I., Patel, J.V., Fearnley, I.M., James, A.M., et al. (2011). Measurement of H<sub>2</sub>O<sub>2</sub> within living *Drosophila* during aging using a ratiometric mass spectrometry probe targeted to the mitochondrial matrix. *Cell Metab.* *13*, 340–350.
- Davidson, S.M., Yellon, D., and Duchon, M.R. (2007). Assessing mitochondrial potential, calcium, and redox state in isolated mammalian cells using confocal microscopy. *Methods Mol. Biol.* *372*, 421–430.
- Jewett, J.C., and Bertozzi, C.R. (2010). Cu-free click cycloaddition reactions in chemical biology. *Chem. Soc. Rev.* *39*, 1272–1279.
- Jucker, B.M., Dufour, S., Ren, J., Cao, X., Previs, S.F., Underhill, B., Cadman, K.S., and Shulman, G.I. (2000). Assessment of mitochondrial energy coupling *in vivo* by <sup>13</sup>C/<sup>31</sup>P NMR. *Proc. Natl. Acad. Sci. USA* *97*, 6880–6884.
- Karamanlidis, G., Lee, C.F., Garcia-Menendez, L., Kolwicz, S.C., Jr., Suthammarak, W., Gong, G., Sedensky, M.M., Morgan, P.G., Wang, W., and Tian, R. (2013). Mitochondrial complex I deficiency increases protein acetylation and accelerates heart failure. *Cell Metab.* *18*, 239–250.
- Karver, M.R., Weissleder, R., and Hilderbrand, S.A. (2012). Bioorthogonal reaction pairs enable simultaneous, selective, multi-target imaging. *Angew. Chemie* *51*, 920–922, S920/921–S920/912.
- Kolb, H.C., Finn, M.G., and Sharpless, K.B. (2001). Click chemistry: diverse chemical function from a few good reactions. *Angew. Chem. Int. Ed. Engl.* *40*, 2004–2021.
- Murphy, M.P. (2009). How mitochondria produce reactive oxygen species. *Biochem. J.* *417*, 1–13.
- Nicholls, D.G., and Ferguson, S.J. (2013). *Bioenergetics 4* (London: Academic Press).
- Perry, S.W., Norman, J.P., Barbieri, J., Brown, E.B., and Gelbard, H.A. (2011). Mitochondrial membrane potential probes and the proton gradient: a practical usage guide. *Biotechniques* *50*, 98–115.
- Perry, R.J., Zhang, D., Zhang, X.M., Boyer, J.L., and Shulman, G.I. (2015). Controlled-release mitochondrial protonophore reverses diabetes and steatohepatitis in rats. *Science* *347*, 1253–1256.
- Porteous, W.K., James, A.M., Sheard, P.W., Porteous, C.M., Packer, M.A., Hyslop, S.J., Melton, J.V., Pang, C.-Y., Wei, Y.-H., and Murphy, M.P. (1998). Bioenergetic consequences of accumulating the common 4977-bp mitochondrial DNA deletion. *Eur. J. Biochem.* *257*, 192–201.
- Porteous, C.M., Logan, A., Evans, C., Ledgerwood, E.C., Menon, D.K., Aigbirhio, F., Smith, R.A.J., and Murphy, M.P. (2010). Rapid uptake of lipophilic triphenylphosphonium cations by mitochondria *in vivo* following intravenous injection: implications for mitochondria-specific therapies and probes. *Biochim. Biophys. Acta* *1800*, 1009–1017.
- Porteous, C.M., Menon, D.K., Aigbirhio, F.I., Smith, R.A.J., and Murphy, M.P. (2013). P-glycoprotein (Mdr1a/1b) and breast cancer resistance protein (Bcrp) decrease the uptake of hydrophobic alkyl triphenylphosphonium cations by the brain. *Biochim. Biophys. Acta* *1830*, 3458–3465.
- Rideout, D. (1994). Self-assembling drugs: a new approach to biochemical modulation in cancer chemotherapy. *Cancer Invest.* *12*, 189–202, discussion 268–269.
- Ross, M.F., Kelso, G.F., Blaikie, F.H., James, A.M., Cochemé, H.M., Filipovska, A., Da Ros, T., Hurd, T.R., Smith, R.A.J., and Murphy, M.P. (2005). Lipophilic triphenylphosphonium cations as tools in mitochondrial bioenergetics and free radical biology. *Biochemistry (Mosc.)* *70*, 222–230.
- Ross, M.F., Da Ros, T., Blaikie, F.H., Prime, T.A., Porteous, C.M., Severina, I.I., Skulachev, V.P., Kjaergaard, H.G., Smith, R.A.J., and Murphy, M.P. (2006). Accumulation of lipophilic dications by mitochondria and cells. *Biochem. J.* *400*, 199–208.
- Ross, M.F., Prime, T.A., Abakumova, I., James, A.M., Porteous, C.M., Smith, R.A.J., and Murphy, M.P. (2008). Rapid and extensive uptake and activation of hydrophobic triphenylphosphonium cations within cells. *Biochem. J.* *411*, 633–645.
- Rotenberg, S.A., Calogeropoulou, T., Jaworski, J.S., Weinstein, I.B., and Rideout, D. (1991). A self-assembling protein kinase C inhibitor. *Proc. Natl. Acad. Sci. USA* *88*, 2490–2494.
- Sack, M.N. (2006). Exploring mitochondria in the intact ischemic heart: advancing technologies to image intracellular function. *Circulation* *114*, 1452–1454.
- Smith, R.A.J., Hartley, R.C., and Murphy, M.P. (2011). Mitochondria-targeted small molecule therapeutics and probes. *Antioxid. Redox Signal.* *15*, 3021–3038.
- Smith, R.A.J., Hartley, R.C., Cochemé, H.M., and Murphy, M.P. (2012). Mitochondrial pharmacology. *Trends Pharmacol. Sci.* *33*, 341–352.
- Sterky, F.H., Hoffman, A.F., Milenkovic, D., Bao, B., Paganelli, A., Edgar, D., Wibom, R., Lupica, C.R., Olson, L., and Larsson, N.G. (2012). Altered dopamine metabolism and increased vulnerability to MPTP in mice with partial deficiency of mitochondrial complex I in dopamine neurons. *Hum. Mol. Genet.* *21*, 1078–1089.
- Wallace, D.C., Fan, W., and Procaccio, V. (2010). Mitochondrial energetics and therapeutics. *Annu. Rev. Pathol.* *5*, 297–348.